






A protocol for karyotyping and genetic editing of induced pluripotent stem cells with homology-directed repair mediated CRISPR/Cas9

Silvana Lobo^{1,2} , Rita Barbosa-Matos¹ , Sofia Dória³ , Ana Maria Pedro¹ , Ana Brito¹, Daniel Ferreira¹  and Carla Oliveira^{1,4,5,*} 

¹i3S—Instituto de Investigação e Inovação em Saúde, University of Porto, Porto, 4200-135, Portugal

²ICBAS—Instituto de Ciências Biomédicas Abel Salazar, University of Porto, Porto, 4050-313, Portugal

³Genetics Unit, Department of Pathology, Faculty of Medicine, University of Porto, Porto, 4200-319, Portugal

⁴IPATIMUP—Institute of Molecular Pathology and Immunology of the University of Porto, Porto, 4200-135, Portugal

⁵FMUP—Faculdade de Medicina, University of Porto, Porto, 4200-319, Portugal

*Corresponding author. i3S—Instituto de Investigação e Inovação em Saúde, University of Porto, Rua Alfredo Allen, 208, Porto, 4200-135, Portugal. Tel: +351 225570785; E-mail: carlaol@i3s.up.pt

Abstract

CRISPR/Cas9-mediated homology-directed repair (HDR) allows precise gene editing, but its efficiency remains low for certain cell types, such as human induced pluripotent stem cells (hiPSCs). In this study, we aimed to introduce the CTNNA1: c.2023C>T (p.Q675*) genetic alteration, which is associated with Hereditary Diffuse Gastric Cancer, into hiPSCs using CRISPR/Cas9. We designed a single-guide RNA targeting the alteration site and a single-stranded oligonucleotide donor DNA template for HDR-based repair. Herein, we report the successful introduction of the CTNNA1: c.2023C>T homozygous alteration in one hiPSC line, which resulted in severe phenotypic changes, including impaired colony formation and cell proliferation. Additionally, we established a straightforward protocol to assess hiPSCs karyotype integrity, ensuring the chromosomal stability required for the gene-editing process. This protocol involves routine G-banding analysis that is required for regular quality controls during handling of hiPSCs. This study demonstrates an efficient approach to precisely edit hiPSCs by CRISPR/Cas9 and highlights the essential role of CTNNA1 expression in maintaining hiPSC viability. Our methodology provides a valuable framework for modeling disease-associated alterations in human-derived cellular models that can be reproduced for other genes and other types of cell lines.

Keywords: CRISPR/Cas9; HDR; hiPSCs; precise genetic editing; karyotyping; CTNNA1

Introduction

Recent advances in genome editing have revolutionized molecular biology in the past decade, with CRISPR/Cas9 emerging as a powerful tool for precise genetic manipulation. This editing technique, originally derived from bacterial adaptive immune system, allows for highly specific DNA targeting and the introduction of specific genetic alterations in the correct site. Being so versatile, CRISPR/Cas9 has become the method of choice for researchers studying gene function, disease modeling, and developing therapeutic strategies in various biological systems, including human cells [1, 2].

Genetic editing by CRISPR/Cas9 occurs due to two major DNA repair pathways, non-homologous end joining (NHEJ) and homology-directed repair (HDR). When Cas9 induces a double-strand break (DSB), NHEJ, the predominant pathway, quickly repairs the DSB, often introducing small insertions or deletions (indels) in the DSB region that can disrupt gene function [3]. This makes NHEJ very useful for gene knockout applications, where precision is not the main goal. In contrast, HDR, which occurs less frequently, uses a homologous DNA template to repair the DSB, allowing highly precise gene editing at the single-base level. Therefore, HDR is the best approach for precise introduction of specific genetic alterations

such as point mutations or corrections [4]. Achieving high efficiency in HDR-mediated CRISPR/Cas9 remains challenging [5] and over the past years, researchers have optimized CRISPR/Cas9 protocols to improve HDR efficacy [6]. Some of the strategies included optimizing the length and understanding the maximum conversion tract of HDR DNA donor templates [7–9]. Furthermore, strategies including a PAM silent alteration have shown to improve editing efficiency by preventing Cas9 re-cutting at the PAM site [10]. In particularly hard-to-edit cell types, such as human induced pluripotent stem cells (hiPSCs), these optimizations can be imperative to achieve a good efficiency in CRISPR/Cas9 precise gene editing.

HiPSCs research achieved a lot of success since their discovery in 2006 by Shinya Yamanaka [11]. These cells are derived by reprogramming adult somatic cells into a pluripotent state, which in turn, allows them to be differentiated virtually into any type of human cell [11]. Besides being an excellent research model due to their ability to give rise to different tissues, they have been considered a promising strategy for regenerative therapy, personalized human genetics, pharmacogenomics, and drug-screening studies [12, 13]. Particularly for rare diseases research, the use of hiPSCs is highly valuable to overcome many of

Received: 13 November 2024; **Revised:** 30 January 2025; **Editorial decision:** 21 February 2025; **Accepted:** 26 February 2025

© The Author(s) 2025. Published by Oxford University Press.

This is an Open Access article distributed under the terms of the Creative Commons Attribution-NonCommercial License (<https://creativecommons.org/licenses/by-nc/4.0/>), which permits non-commercial re-use, distribution, and reproduction in any medium, provided the original work is properly cited. For commercial re-use, please contact reprints@oup.com for reprints and translation rights for reprints. All other permissions can be obtained through our RightsLink service via the Permissions link on the article page on our site—for further information please contact journals.permissions@oup.com.

their associated challenges, such as the establishment of cell lines that mimic the genetic background of affected individuals, which not only avoids some of the ethical concerns associated with the use of embryonic stem cells but also decreases the use of animal models for research purposes [14]. Especially for cancer research, hiPSCs allows to study the biological and molecular part of tumor initiation and development, and enables the modeling of genetic alterations that drive cancer progression [15]. Despite all these advantages, hiPSCs cell culture conditions are associated with genomic instability [16]. Therefore, it is important to guarantee the quality and integrity of these cells when in culture for long-term. G-banded karyotyping allows to detect numerical and structural chromosomal abnormalities and is a straightforward and low-cost technique [17]. If any abnormality is detected, hiPSCs should be discarded.

In this study, we aimed to establish a protocol to introduce a disease-relevant single nucleotide alteration in hiPSCs using HDR-mediated CRISPR/Cas9, while also optimizing hiPSC characterization methods, such as the G-band karyotyping protocol. For this, we selected the CTNNA1 gene. CTNNA1 encodes α E-catenin, a key player in the cadherin-catenin adhesion complex. Germline truncating alterations in CTNNA1 have been associated with Hereditary Diffuse Gastric Cancer (HDGC), a very aggressive and rare hereditary cancer syndrome that predisposes for development of early onset diffuse gastric cancer and invasive lobular breast cancer [18, 19]. In our approach, we introduced one of the truncating CTNNA1 variants associated with HDGC, the CTNNA1: c.2023C>T nonsense variant [20], that causes a premature termination codon in CTNNA1 exon 15. We used a single-guide RNA (sgRNA) targeting the site of the alteration, alongside a single-stranded oligonucleotide (ssODN) donor DNA template designed for HDR-based DNA repair. We were further successful in implementing a G-band karyotyping protocol for hiPSCs culture maintenance, that could be easily performed in different labs.

We report an efficient HDR-mediated CRISPR/Cas9 strategy for precise gene editing in hiPSCs and provide novel insights into the role of CTNNA1 in non-differentiated cells. Our findings further demonstrate that introducing a nonsense alteration in CTNNA1 in a homozygous state results in severe phenotypic changes, suggesting a role for α E-catenin in maintaining stable hiPSCs. This methodology can be applied broadly to investigate gene function in hiPSCs and model disease-relevant alterations in a controlled and reproducible manner, consistent with good handling of hiPSCs cultures.

Methodology

Cell maintenance

Gibco™ episomal hiPSC line (#A18945) was purchased from ThermoFisher (Waltham, MA, USA) and is a viral-integration-free hiPSC line, adapted to feeder-free, serum-free culture conditions. Cells were maintained in Matrigel-coated six-well plates (Corning® Matrigel® hESC-qualified Matrix, #354277, Corning, NY, USA) and seeded in mTeSR™1 medium (#85850, StemCell Technologies, Vancouver, Canada) under 37°C and 5% CO₂ in a humidified incubator.

Immunofluorescence for phenotypic assessment of pluripotent markers in hiPSCs

Immunofluorescence analysis was performed to confirm the pluripotent state of Gibco™ episomal hiPSC line. For that we used the ES/iPSC Cell Characterization Kit from EMD Millipore (#SCR001; Burlington, MA, USA). Cells grew in glass coverslips for

3 days. Next, cells were washed in 1× PBS and fixed in 4% PFA (v/v) (Merck, Darmstadt, Germany) for 20 min at room temperature (RT). All subsequent cell washes were performed using TBST (TBS with 0.1% Tween-20). Cells were incubated in 0.2% TritonX-100 (v/v) (Sigma, St Louis, MO, USA) in 1× PBS (5 min at RT) to permeabilize cell membrane. Afterwards, cells were incubated in the blocking solution (4% normal goat serum in 1× PBS for 30 min at RT), and subsequently, primary antibodies from the characterization kit were added: mouse anti-SSEA-1, mouse anti-SSEA-4, mouse anti-TRA-1-60, and mouse anti-TRA-1-81 (1:50; 1 h incubation at RT). Secondary antibodies goat anti-mouse IgGs conjugated with Alexa Fluor 488 or Alexa Fluor 546 from Invitrogen were used (1:250; 1 h incubation at RT). Finally, cells were incubated for 10 min at RT in 1 µg/ml DAPI (#28718-90-3, Sigma-Aldrich, Poole, UK) in 1× PBS and coverslips were mounted in Vectashield anti-fade mounting media (Vector Laboratories, Burlingame, CA, USA). Fluorescence was measured using the Leica SP5 confocal microscope and analysed using Leica Application Suite X (Leica, Wetzlar, Germany).

Immunofluorescence for adherens' junction molecules

Immunofluorescence analysis was performed to determine α E-catenin and E-cadherin protein expression in hiPSCs. Cells were plated and allowed to grow for 3 days in glass coverslips. Subsequently, media was discarded, cells were washed in 1× PBS and fixed in 4% PFA (v/v). Afterwards, NH₄Cl 50 mM (v/v) in 1× PBS was added to decrease cell autofluorescence, cells were washed, and 0.2% TritonX-100 (v/v) in 1× PBS was added. Next, 5% BSA (w/v) in 1× PBS was used as blocking solution and, subsequently, cells were incubated at 4°C overnight in a humidified chamber in α E-catenin and E-cadherin primary antibodies: mouse anti α -Catenin monoclonal antibody alpha-CAT-7A4 (1:200; ThermoFisher) or rabbit anti E-cadherin monoclonal antibody 24E10 (1:100; Cell Signalling). Further incubation with secondary antibodies was performed: Goat anti-Mouse or Goat anti-Rabbit IgG (H+L) Highly Cross-Adsorbed Secondary Antibody, Alexa Fluor™ Plus 647 (1:500, 2 h incubation at room temperature). In the end, cells were incubated for 5 min in 1 µg/ml DAPI and coverslips were mounted in Vectashield. Fluorescence was measured using the Leica SP5 confocal microscope and analyzed using Leica Application Suite X (Leica, Wetzlar, Germany).

Karyotype analysis for hiPSC

Chromosome slides were prepared and GTL-banding was performed using Leishman stain (#L6254, Sigma) in accordance with established laboratory protocols. To analyze hiPSCs, a minimum of 20 metaphases were analyzed, following the guidelines of the International System for Human Cytogenomic Nomenclature (ISCN) [21]. Metaphases were karyotyped using the CytoVision/v3.932 software (Applied Imaging Cytovision). The detailed protocol for this technique is available in the [Supplementary material](#).

Design of sgRNA and a single-stranded oligonucleotide DNA donor template

sgRNA was designed with the WTSI Genome Editing (WGE) online tool (<https://www.sanger.ac.uk/tool/wge-crispr-design-tool/>). The gRNA was designed to target CTNNA1 exon 15, specifically to perform the nonsense CTNNA1: c.2023C>T (p.Q675*) variant in a homozygous state. The gRNA was purchased from Alfacene (Carcavelos, Portugal) as forward and reverse sequences for further annealing to create a double stranded sgRNA: 5'-CACCGGATCATGGCTCAGCTTCCCC-3' (forward) and 5'-AAACGGGAAGCT

GAGCCATGATCC-3' (reverse). Underlined nucleotides correspond to the BbsI digestion motif, for proper ligation to the BbsI digested plasmid during the cloning protocol. A ssODN donor template was designed containing the desired alteration, as well as a silent mutation on the PAM site (CTNNA1: c.2034G>A; p. Q678=), and was purchased from IDT (Coralville, IA, USA): 5'-GCTTCTGATCACAGGCGA TCATGGCTTAGCTTCCCCAAGAGCAAAAAGCGAAGATTGCGGAAC AGGTGGCCAGCTTCCAGGAAGAAAAGAGCAAGCTGGATGCTGAA GTGTCCAAATGGGACGACAG-3'. This further contained an Alt-R HDR modification variation from IDT to improve stability upon delivery to cells.

The sgRNA was cloned into the pSpCas9(BB)-2A-GFP (PX458) vector from Addgene (#48138; Watertown, MA, USA), which contains the Cas9 gene from *S. pyogenes*, a GFP selection marker cassette and the PX458 vector backbone. 1 µg of pSpCas9(BB)-2A-GFP (PX458) vector was digested using 10 units of the BbsI restriction enzyme from New England Biolabs (#R0539S; Ipswich, MA, USA). sgRNA forward and reverse sequences were annealed to form a double chain sequence and ligated to the vector using 200 units of T4 DNA ligase from New England Biolabs (#M0202S). A 1:1 vector: sgRNA ligation ratio was used and ligation was performed at 16°C overnight. Two microliter of ligation reaction were further transformed in 50 µl of competent *E. coli* cells (Stbl3). Three colonies were picked for subsequent sanger sequencing to confirm the insertion of the sgRNA. One positive colony was then expanded and the QIAGEN Maxiprep kit (#12362, Hilden, Germany) was used to isolate highly pure plasmids, following the manufacturer's instructions.

Cas9 plasmid and ssODN donor template electroporation

The plasmid containing the Cas9 and the sgRNA, as well as the ssODN donor template was delivered to hiPSCs through electroporation. Briefly, fresh mTeSRTM1 medium containing 10 mM ROCK inhibitor was added to hiPSCs for one hour. Afterwards, cells were detached and resuspended to a single cell state. Cells were counted and 6×10^6 cells were resuspended in nucleofector reagent from the P3 Primary Cell 4D-NucleofectorTM X Kit from Lonza (Basilea, Switzerland). Cells were then placed carefully in a nucleocuvette vessel to avoid the presence of bubbles and were subsequently electroporated in the Lonza 4D-nucleofector system. After electroporation, the nucleocuvette vessels containing the cells were incubated at 37°C for 15 min. Finally, electroporated cells were plated in Matrigel-coated plates containing fresh mTeSRTM1 medium with 10 mM ROCK inhibitor. After 24 h, 10 mM ROCK inhibitor was retrieved from cells and these were allowed to grow before cell sorting. For the optimization step of the electroporation protocol, three programs already used in human iPSCs were tested (CM-100, CM-130, CB150) [22–24]. Only the most successful electroporation program was used in the CRISPR/Cas9 experiment, namely the CM-130 program.

FACS cell sorting

After electroporation, cells were allowed to recover and grow for 72 h. Before starting the cell sorting protocol, cells were incubated in 10 mM ROCK inhibitor for 1 h. Afterwards, media was removed, cells were detached and resuspended in mTeSRTM1 with 10 mM ROCK inhibitor. Next, cells were centrifuge at 200 g for 10 min and resuspended in 400 µl of mTeSRTM1 containing 10 mM ROCK inhibitor. Cell suspension was filtered using a 40 µm pore filter and placed in a sterile cytometer tube. Cells were then sorted for GFP positive expression using the FACS Aria II cell sorter from BD Biosciences (Franklin Lakes, NJ, USA). Finally, GFP+ cells were plated in a 10 cm Matrigel-coated petri dish containing fresh

mTeSRTM1 medium with 10 mM ROCK inhibitor. After 24 h, cells were retrieved from the 10 mM ROCK inhibitor and allowed to grow. GFP positive expression was analyzed using the ZOETM Fluorescent Cell Imager from Bio-Rad (Hercules, CA, USA).

Genotyping of CRISPR/Cas9 hiPSC clones

Clones derived from cell sorting were isolated and allowed to grow separately in 12-well plates. Afterwards, gDNA was extracted using the NZY Tissue gDNA Isolation kit from NZYTech (Lisbon, Portugal), according to the manufacturer's protocol. DNA concentration and quality was measured with NanoDrop[®] One UV-Vis. DNA quality was assessed by Abs260/Abs280 ratio above 1.80. The extracted genomic DNA was then used to perform a set of genotyping PCRs. Multiplex PCR kit from Qiagen was used to amplify CTNNA1 exon 15 by using primers in the adjacent intronic areas. A short ~400 bp and a long ~2 Kb sequence spanning from intron 14 to intron 15 were analyzed. The primers used for the short analysis were the following: 5'-ACCTATGCCACAGATTGCCT-3' (forward); 5'-GCCCTCAGATT GGAGTAG-3' (reverse). The primers used for the long analysis were the following: 5'-AGAAAGCCAGTCAGGCCAT-3' (forward); 5'-GAGGCTCCAGATTAGGACC-3' (reverse). PCR products were analyzed by electrophoresis through a 1.5% agarose gel with GreenSafe premium dye from NZYTech and a Gel DocTM XR+ Gel Documentation System from Bio-Rad was used to reveal the electrophoresis. In clones with more than one band, bands were cut and DNA was purified using the illustraTM triplePrep kit from GE HealthCare (Chicago, IL, USA). In clones presenting only one band, PCR product was purified with ExoSAP-IT PCR Product Cleanup Reagent from Applied Biosystems (Waltham, MA, USA). All clones were sanger sequenced to confirm the presence or absence of genetic editing using the BigDyeTM Terminator v3.1 Cycle Sequencing Kit from Applied Biosystems and the same genotyping primers, and were analyzed using the Applied Biosystems 3130xl Genetic Analyzer. Samples presenting more than one sequence in the Sanger sequencing file were deconvoluted using the Mutation Surveyor v5.2.0 tool (State College, PA, USA) and manually confirmed.

Results

To test the HDR-mediated CRISPR/Cas9 protocol, we mimicked the CTNNA1: c.2023C>T (p.Q675*) nonsense variant, causing CTNNA1 truncation and CTNNA1 loss-of-function [19, 20]. The entire study workflow is described in Fig. 1.

Characterization of genomic stability and expression of pluripotency markers is essential prior to genomic editing in hiPSCs

Confirming the pluripotency potential of the hiPSC line to be used is the first step before starting genetic editing with the HDR-mediated CRISPR/Cas9 protocol. For this, it is essential to select markers, not only to characterize hiPSCs, but also to monitor pluripotency in cultures over time. We selected TRA-1-60, TRA-1-81 and SSEA-4 as pluripotency markers, and SSEA-1 as a negative control. TRA-1-60 and TRA-1-81 are high-molecular-weight cell surface glycoproteins expressed by human ESCs and hiPSCs. SSEA-4 and SSEA-1 are cell surface antigens, while SSEA-4 is commonly expressed in hiPSCs, SSEA-1 expression is negative in these cells [25].

We used the Gibco Episomal hiPSC Line (A18945, ThermoFisher), derived from the cord blood of a newborn female, confirmed cultures were mycoplasma-free (data not shown), and used immunocytochemistry to characterize the expression of TRA-1-60, TRA-1-81, and SSEA-4 and SSEA-1. This analysis confirmed that the Gibco Episomal hiPSC Line is negative for SSEA-1, while SSEA-4,

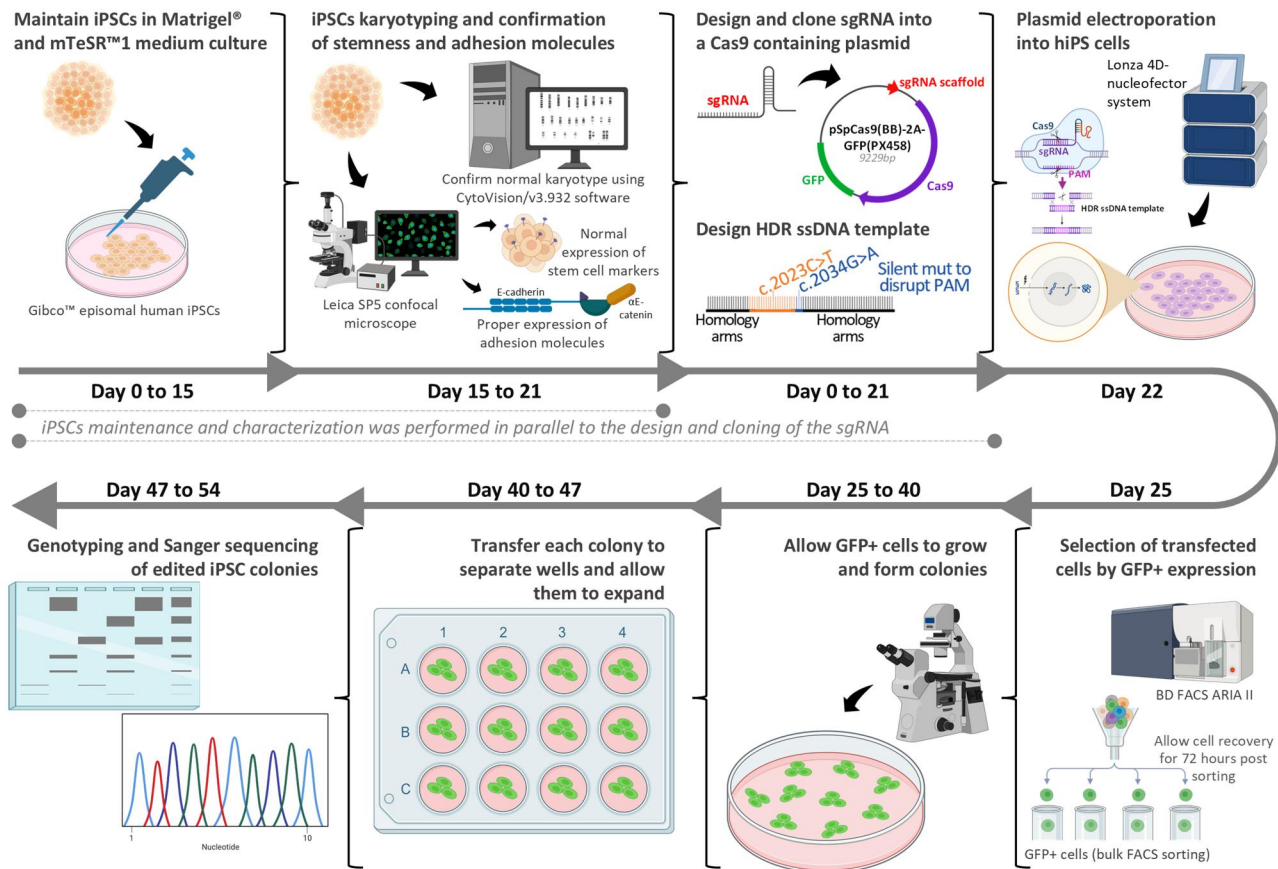


Figure 1. Study design. We introduced the CTNNA1: c.2023C>T (p.Q675*) nonsense variant into hiPSCs. For that, we designed a sgRNA to drive Cas9 into the target location of the c.2023C>T alteration, and a ssODN HDR donor template to be used by cells as a DNA repair template, after Cas9 DSB. We cloned the sgRNA into a pSpCas9(BB)-2A-GFP(PX458), which contains the Cas9 gene and a GFP selection marker. We delivered both the plasmid and the ssODN template to hiPSCs by electroporation and submitted them to FACS cell sorting to select GFP+ cells. Sorted cells were allowed to grow and the new colonies were isolated and genotyped to assess the success of HDR-mediated CRISPR/Cas9 genetic editing.

TRA-1-60, and TRA-1-81 are expressed at the membrane (Fig. 2A). The expression profile of these markers supports the pluripotency of the selected cell line to be used.

Since we wanted to edit the CTNNA1 gene to mimic a genetic alteration predicted to cause CTNNA1 loss of expression, it was important to confirm that the cadherin-catenin adhesion complex was intact, validating the proper expression of αE-catenin, as well as E-cadherin adhesion molecule. We confirmed, by immunohistochemistry, that both αE-catenin and E-cadherin proteins display a membranous expression and are concomitantly expressed in hiPSCs (Fig. 2B).

To assess chromosomal stability and exclude potential chromosomal abnormalities that can occur during hiPSC line culture, we performed the karyotype using GTL-banding. The cytogenetic analysis consisted in the observation of at least 20 metaphases, counting and analyzing the structure of all chromosomes by an experienced cytogeneticist. For all the cells analyzed, a normal female chromosomal complement (46, XX) was observed (Fig. 2C).

Development of an HDR-mediated CRISPR/Cas9 strategy for targeting the CTNNA1: c.2023C>T variant

Proximity to the target mutation site is a priority for optimized sgRNA and ssODN donor template design for efficient editing

To design the sgRNA, we used WGE online tool. Here, we analyzed the presence of Cas9 PAM in the vicinity of the position to

be modified. We identified an “AGG” PAM motif 9 bp downstream of the c.2023 nucleotide. Cas9 is expected to cause a DSB 3-4bp upstream this motif. Thus, the c.2023 nucleotide is expected to be located 5-6bp upstream the DSB site. Previous studies have demonstrated that the efficacy of HDR-mediated CRISPR/Cas9 significantly drops with the increasing distance to the mutation site, with efficacy dropping to half if this distance is longer than 10bp [26]. We designed a 21bp long sgRNA that target the sequence right upstream of the PAM motif mentioned above (Fig. 3A). This sgRNA was selected especially due to its proximity to the mutation target site. The 21bp length for the sgRNA was selected to ensure a favorable on-target specificity, while not increasing the off-target effects.

We next designed a ssODN HDR donor template to be used as a template to correct the DSB caused by Cas9. For this, we used the Alt-R HDR Design Tool (IDT) and further optimized donor DNA templates to improve HDR-mediated CRISPR/Cas9 editing [27]. With this tool, we designed a 127bp long ssODN, containing asymmetric homology arms with 36bp on the PAM-distal arm and 91bp on the PAM-proximal arm of the DSB (Fig. 3B). This ssODN contained the desired alteration (c.2023C>T), as well as a silent alteration in the 2nd nucleotide of the PAM sequence (AGG to AAG). This alteration, CTNNA1: c.2034G>A, is synonymous and does not change αE-catenin amino acid sequence (p.Q678=) (Fig. 3B). Cas9 can be active in cells for several hours, leading to Cas9 recutting after introducing the desired alteration, because it still recognizes the PAM

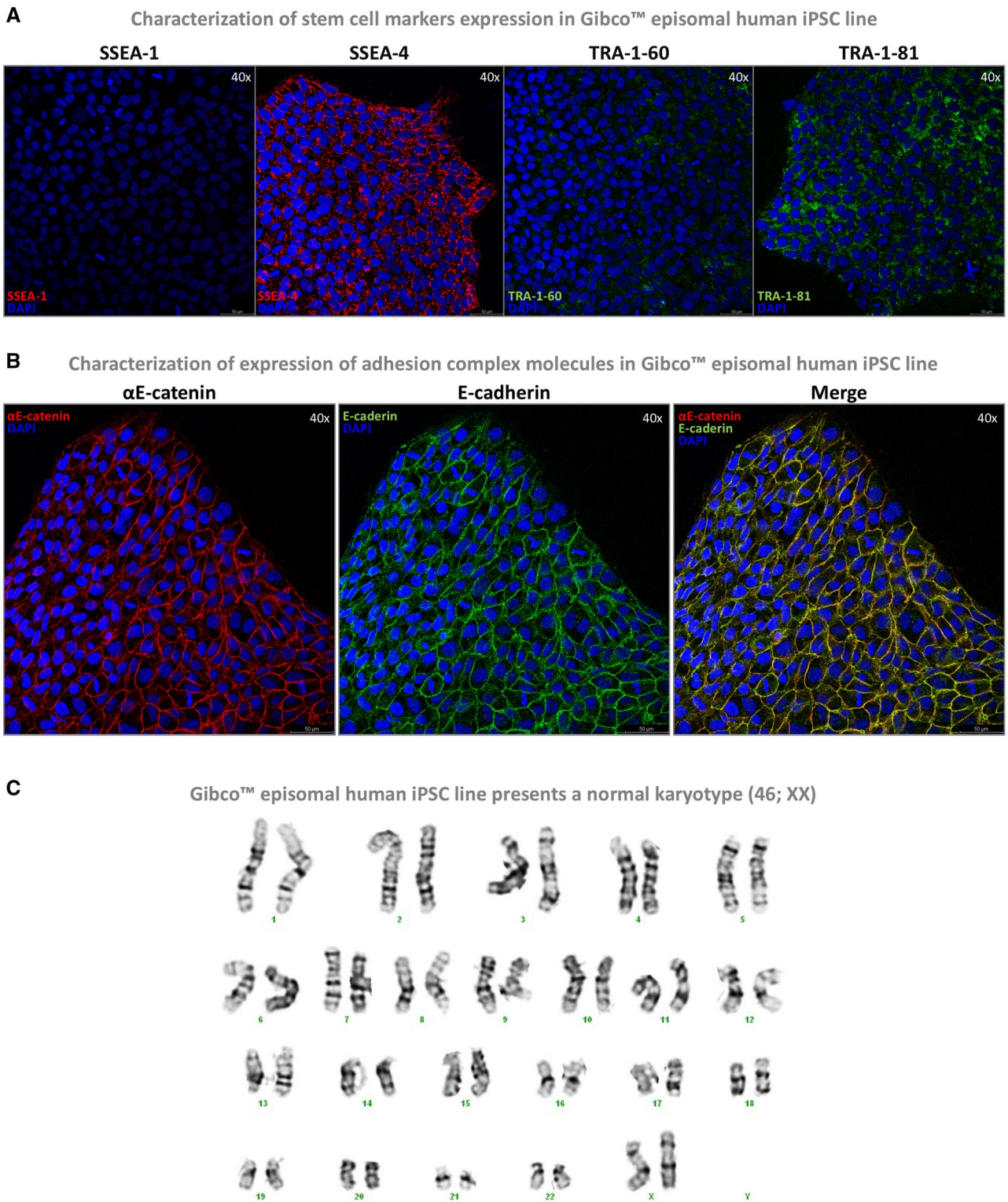


Figure 2. Molecular characterization of wild-type hiPSCs. Immunocytochemistry analysis of the expression of: (A) SSEA-1 (red), SSEA-4 (red), TRA-1-60 (green) and TRA-1-81 (green); (B) α E-catenin (red) and E-cadherin (green). The coloring of DAPI is represented in blue. (C) Karyotype analysis of wild-type hiPSCs.

sequence [28]. The introduction of the PAM silent mutation was intentional, as it leads to non-recognition of the PAM sequence by Cas9, once the ssODN template is integrated, preventing recutting of edited cells.

Validation of off-target effects in HDR-mediated CRISPR/Cas9

One key point of CRISPR/Cas9-mediated genetic editing is the high specificity for the target site. For this, the sgRNA sequence

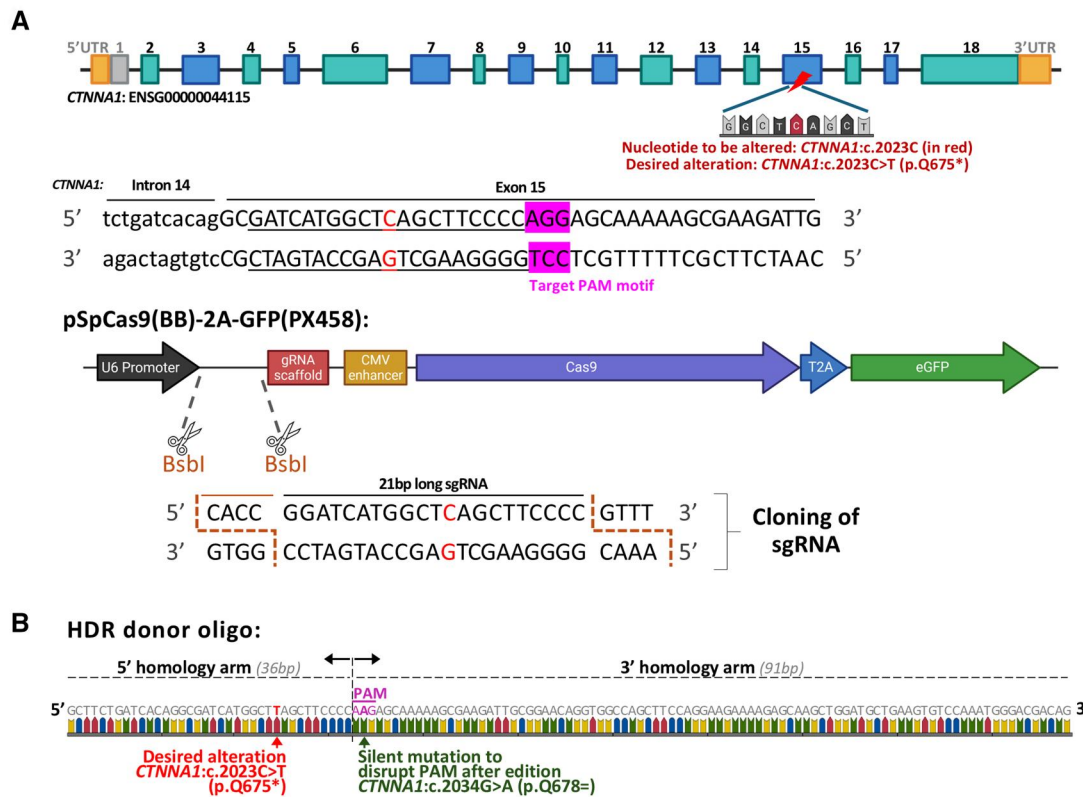


Figure 3. Design and optimization of sgRNA and ssODN donor template for *CTNNA1* editing. **(A)** The WTSI Genome Editing (WGE) online tool was used to design the sgRNA. A BbsI motif was added to the sgRNA sequence in order to properly ligate to PX458 vector after BbsI digestion. **(B)** The ssODN HDR template was designed using the Alt-R HDR Design Tool from IDT. We also followed the guidelines provided by Addgene blog to optimize donor DNA template to improve HDR-mediated CRISPR/Cas9 genetic editing.

must present a low off-target effect. We used the WGE online tool to further identify candidate off-target regions with sequence similarity to the on-target Cas9 site. We identified 241 off-target sites associated with the sgRNA sequence. Of these, 89.1% (215) presented at least four mismatches to the sgRNA sequence, while 25/241 (10.4%) presented three mismatches, significantly impairing the recognition of these regions by the sgRNA [29–31]. One off-target presented only one mismatch (0.4%) to the sgRNA sequence in the most 3' nucleotide of the sequence, right before the PAM site. This off-target site was located in chromosome 5:115390356-115390378, a non-coding intergenic region identified as *CTNNA1P1* [32]. A detailed description of all off-target sites is provided in [Supplementary Table 1](#).

Optimization of electroporation and flow cytometry allows selection of CRISPR-edited hiPSCs using HDR-mediated CRISPR/Cas9

To introduce the Cas9+sgRNA plasmid and the ssODN HDR donor template, we electroporated hiPSCs. For that, we used the P3 Primary Cell 4D-Nucleofector™ X Kit and the 4D-nucleofector system from Lonza. To assess the successful introduction of plasmid DNA using this method, we carried out an optimization step using a GFP+ commercial plasmid (Fig. 4A). Here, we electroporated hiPSCs using three different electroporation programs (CM-100, CM-130, and CB-150) to introduce the pmaxGFP® plasmid, a control commercial vector containing the GFP fluorescent marker. CM-130 electroporation program presented the higher percentage of GFP+ cells (13.5%) when comparing to CM-100 (1.17%) or CB-150 (6.42%) (Fig. 4A). Qualitative analysis of GFP

expression further confirms that CM-130 electroporation program displayed more cells expressing GFP fluorescent marker.

Afterwards, we electroporated the Cas9 plasmid and ssODN donor template under the CM-130 program, and further selected GFP+ cells with FACS sorting. GFP+ cells selection was performed 72 h after electroporation, which allowed cell recovery. Cells were detached to achieve a single cell state and, right after, hiPSCs were sorted for GFP. Our results demonstrate that 2.5% of all cells expressed GFP (Fig. 4B). The 522 GFP+ cells were all plated in one 10 cm Petri dish coated in Matrigel®. For the subsequent 24 h, cells were maintained in mTeSR1 with 10 mM ROCK inhibitor to help single-cells recovering. GFP expression qualitative analysis confirmed expression of GFP in FACS sorted cells.

Genotypic analysis reveals variable editing efficiency and outcomes in hiPSC clones following HDR-mediated CRISPR/Cas9 editing

After FACS sorting, 522 cells were plated in one 10 cm Petri dish, from which 24 clones grew and were selected for colony picking and expansion. For the colony-picking technique, it is crucial that colonies are large and isolated with well-established borders.

Each picked colony was transferred to a new freshly Matrigel® coated well of a 12-well plate using a 10 µl pipette tip, cultured in cell medium with 10 mM ROCK inhibitor. Of the 24 transferred clones, 29% (7/24; clones #7, 9, 14, 15, 19, 21, and 22) did not survive the post-transfer period. The remaining 17 clones were expanded (Fig. 5A), and gDNA was extracted for genotyping analysis (Fig. 1). Our results demonstrate that 47% (8/17) of all clones presented only mutated cells (Fig. 5A and B). One clone (#1) presented both mutated and WT sequences. Of all clones,

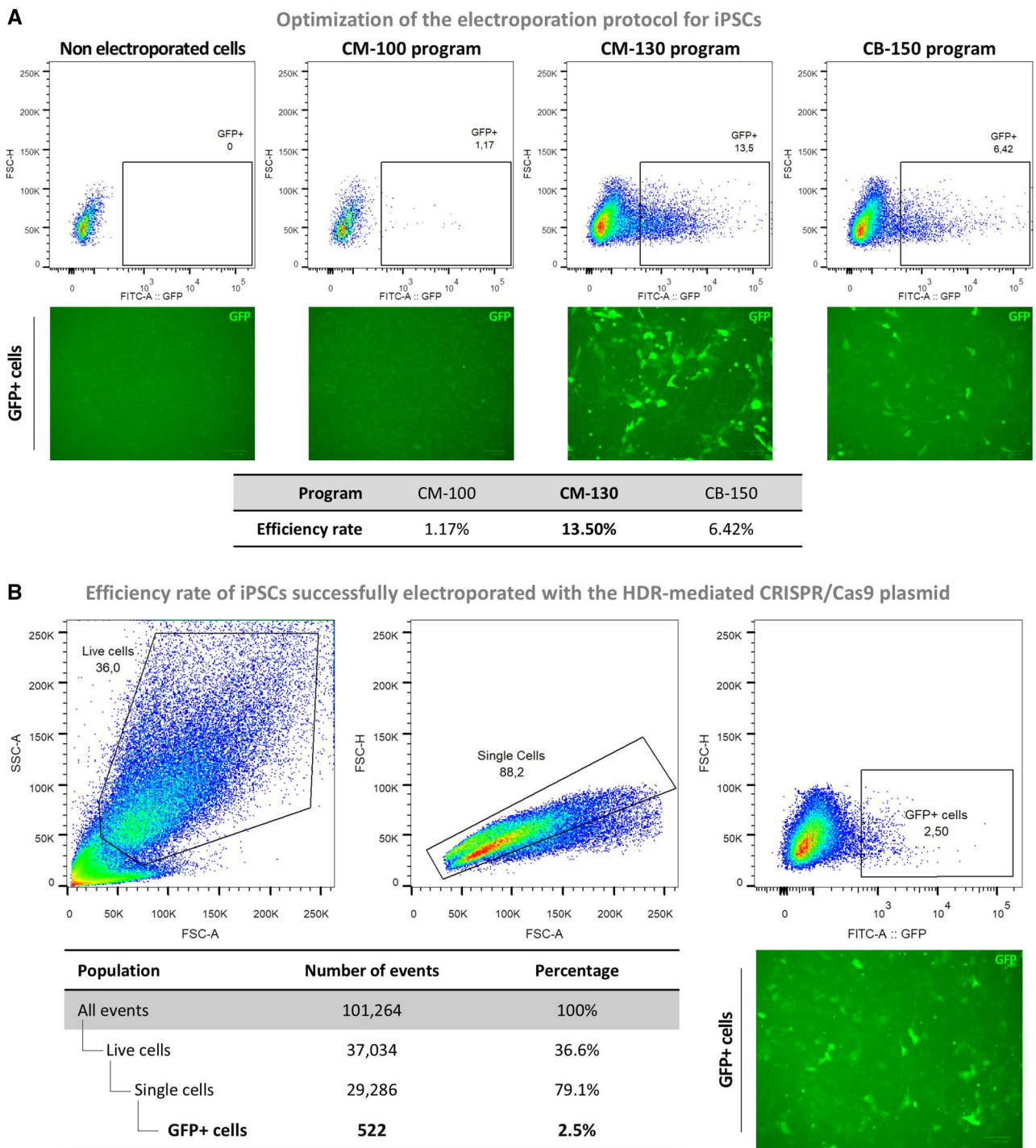


Figure 4. Selection of CRISPR/Cas9 edited hiPSCs. (A) Optimization of the electroporation program for hiPSCs. Graphs represent FACS cell sorting experiments and images represent the respective GFP expression analysis. (B) Selection of GFP+ cells after CRISPR/Cas9 editing. The 1st graph selected the population of cells expected to be alive (live cells); the 2nd graph selected the population of cells expected to be in a singlet state (single cells); the 3rd graph selected the GFP+ cells that were further sorted to a 10 cm petri dish with fresh Matrigel[®] and medium and allowed to grow for the subsequent days. The table follows the same scheme, presenting the quantification of cells and the respective percentage. Image represents the respective GFP expression analysis. Scalebars represent 100 μ m.

the DNA repair mechanism used after Cas9 cutting was HDR in 1/17 (6%) and NHEJ in 8/17 (47%) (Fig. 5A). Clone #8, the only where HDR-mediated DNA repair was achieved, presented in a homozygous state the CTNNA1: c.2023C>T (p.Q675*) target alteration, as well as the PAM silent CTNNA1: c.2034G>A (p.Q678=) that was added to the ssODN HDR donor template to prevent Cas9 recutting. Three clones (#16, 20, and 23) also presented the

PAM silent alteration, but were WT for the c.2023C>T target alteration. This indicates that the HDR template was integrated, however, the c.2023C>T desired alteration did not occur (Fig. 5A). Regarding the NHEJ-mediated DNA repaired clones, a pleiotropy of different indels could be observed (Fig. 5A and B). Clone #1 presented a 13bp deletion, as well as two different insertions of ~500bp and ~400bp, respectively. Clones #2, 12, 13, and 24 all

A

522 GFP+ cells were FACS sorted to a 10cm Matrigel® coated plate → 24 colonies were individually transferred to 12-well plates → 17/24 colonies survived and gDNA was genotyped

Clone no.*	Sequences found (N)	Sequence 1	Sequence 2	Other sequences	Predicted αE-cat expression	Phenotype	PAM mutated?
1	4	WT	13bp deletion (Frameshift alteration; disrupts the ORF in <i>CTNNA1</i> exon 15)	~500bp and ~400 insertions (breakpoints not determined) ⁵	Normal	Normal	NO
2	2	3bp deletion (In-frame deletion of 3bp in exon 15; does not disrupts the ORF)	13bp deletion (Frameshift alteration; disrupts the ORF in <i>CTNNA1</i> exon 15)	-	Normal (1 amino acid shorter protein)	Normal	NO
3	1	WT	-	-	Normal	Normal	NO
4	1	WT	-	-	Normal	Normal	NO
5	2	1bp del (Frameshift alteration; disrupts the ORF in <i>CTNNA1</i> exon 15)	238bp deletion (In-frame deletion of 24bp in exon 15; does not disrupts the ORF)	-	Normal (8 amino acid shorter protein)	Normal	NO
6	2	1bp del (Frameshift alteration; disrupts the ORF in <i>CTNNA1</i> exon 15)	238bp deletion (In-frame deletion of 24bp in exon 15; does not disrupts the ORF)	-	Normal (8 amino acid shorter protein)	Normal	NO
8	1	<i>CTNNA1</i> :c.2023C>T nonsense alteration	-	-	Loss-of-expression	Severe cell adhesion and proliferation loss	YES
10	1	WT	-	-	Normal	Normal	NO
11	1	WT	-	-	Normal	Normal	NO
12	2	9bp deletion (In-frame deletion of 9bp in exon 15; does not disrupts the ORF)	2bp deletion (Frameshift alteration; disrupts the ORF in <i>CTNNA1</i> exon 15)	-	Normal (3 amino acid shorter protein)	Normal	NO
13	2	9bp deletion (In-frame deletion of 9bp in exon 15; does not disrupts the ORF)	8bp deletion (Frameshift alteration; disrupts the ORF in <i>CTNNA1</i> exon 15)	-	Normal (3 amino acid shorter protein)	Normal	NO
16	1	WT	-	-	Normal	Normal	YES
17	1	WT	-	-	Normal	Normal	NO
18	2	6bp deletion + 226bp insertion (Frameshift out-of-frame alteration; disrupts the ORF)	1098bp deletion (out-of-frame large deletion; only disrupts the ORF deep into <i>CTNNA1</i> last exon)	-	Normal (31 amino acid shorter protein)	Normal	NO
20	1	WT	-	-	Normal	Normal	YES
23	1	WT	-	-	Normal	Normal	YES
24	2	9bp deletion (In-frame deletion of 9bp in exon 15; does not disrupts the ORF)	17bp deletion (Frameshift alteration; disrupts the ORF in <i>CTNNA1</i> exon 15)	-	Normal (3 amino acid shorter protein)	Normal	NO

*Only clones surviving colony transfer are depicted; ⁵The two large insertions from clone #1 are highlighted in (B).

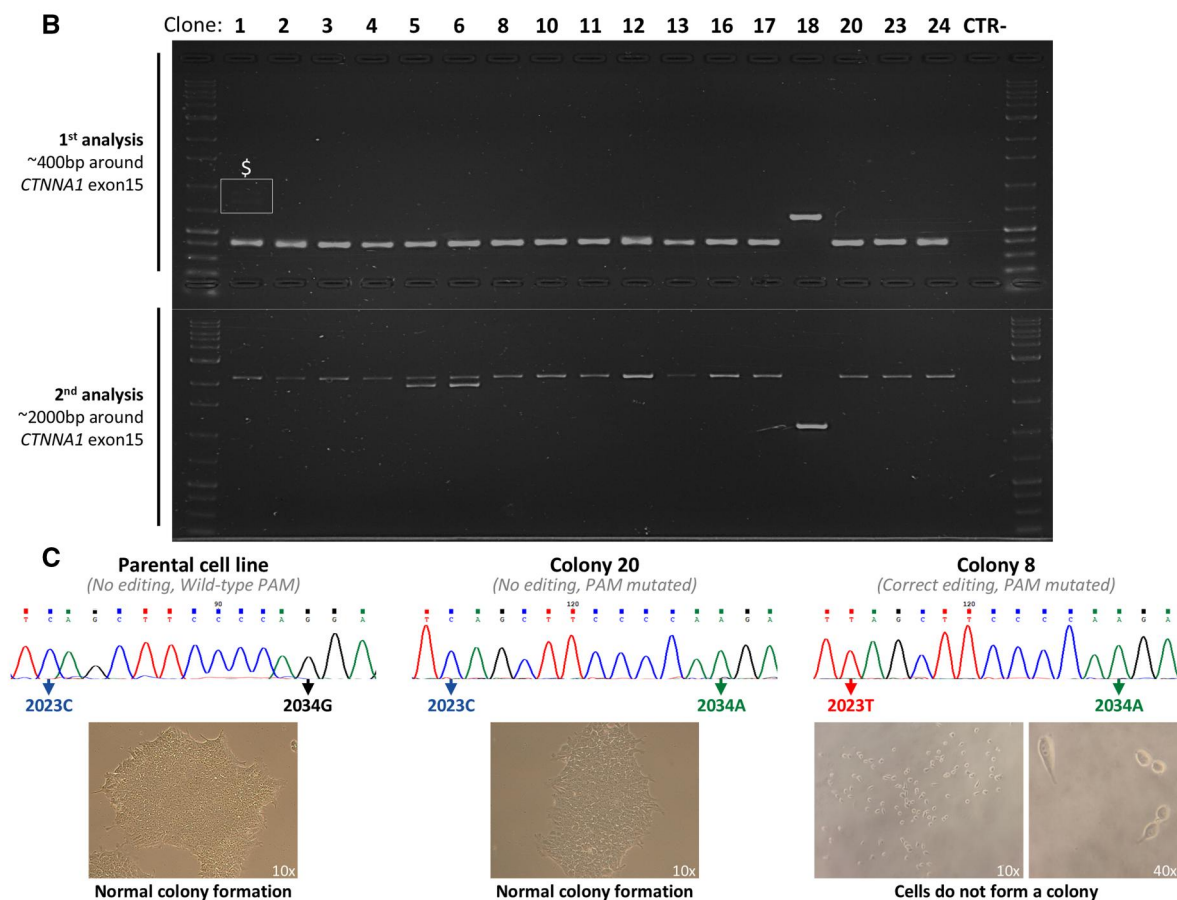


Figure 5. Characterization of CRISPR/Cas9 genetic edited hiPSCs. (A) Detailed description of the clones that were successfully genotype for the presence/absence of HDR-mediated CRISPR/Cas9 genetic alterations; (B) Electrophoresis displaying the genotyping of the *CTNNA1* sequence in the vicinity of the DSB Cas9 site of the clones; (C) Sanger sequencing and macroscopic phenotype of WT hiPSCs, hiPSCs presenting only the homozygous silent PAM alteration (c.2034G>A), and hiPSCs presenting both the homozygous target alteration (c.2023C>T) and the homozygous silent PAM alteration (c.2034G>A).

presented two different sequences containing small deletions, with one being in-frame and one frameshift. Clones #5 and 6 presented two different sequences, one containing a 1 bp deletion causing a frameshift alteration, and one 238 bp-long deletion that leads to the in-frame deletion of 24 bp in exon 15. Moreover, clone #18 presents one 226 bp out-of-frame large insertion and one 1098 bp large deletion. In this case, the large deletion leads to a premature stop codon only in the end of exon 18, *CTNNA1* last exon, that is predicted to escape nonsense mediated mRNA decay, thus leading to a shorter but functional protein [33, 34]. Of all successfully edited clones, only clone #8 presented a drastic change in cell phenotype, while all other clones revealed no phenotypic alterations (Fig. 5C). These results further demonstrated that the PAM silent homozygous alteration, alone, does not cause any phenotype changes. Furthermore, 29% (5/17) of all clones (#3, 4, 10, 11, and 17) did not presented any genetic edition, either in the target site nor in the PAM motif (Fig. 5A and B).

Genotyping analysis of the *CTNNA1P1* off-target site revealed that off-target Cas9 cleavage occurred in 63% (10/16; clone #13 was not successfully sequenced) of all clones (Supplementary Fig. 1). Herein, eight clones (#1, 2, 8, 12, 16, 18, 20, 23) presented two sequences of the *CTNNA1P1* off-target site, one WT and one containing small indels. Furthermore, clones #5 and 6 contained only a 150 bp deletion around the off-target site, and no WT sequence was found.

hiPSCs require an intact *CTNNA1* locus for colonies viability and proliferation

We performed a microscopic analysis on the edited clones and our results demonstrated that only the nonsense *CTNNA1* variant c.2023C>T (p.Q675*) was deleterious to hiPSCs. This homozygous genetic alteration resulted in a severe loss of adhesion phenotype and in a critical impact in cell viability, incompatible with colony survival. Ultimately, this clone was not viable due to impaired cell proliferation, resulting in the total loss of this isogenic hiPSC line (Fig. 5B and C). Furthermore, all other edited clones presented a phenotype identical to the WT hiPSC line. This was expected since all edited clones presented at least a WT or an in-frame mutated sequence that is predicted to not disrupt the open reading frame of *CTNNA1/αE-catenin*.

Discussion

In the current study, we report the use of HDR-mediated CRISPR/Cas9 to cause a specific nucleotide alteration (*CTNNA1*: c.2023C>T) in hiPSCs in less than 2 months, as well as a fully optimized unexpensive karyotyping protocol for proper iPSCs culture maintenance. The correct characterization of hiPSC cultures regarding genomic instability and pluripotency is mandatory before their experimental applications. *In vitro* culture of hiPSCs and their associated genetic reprogramming can cause chromosomal abnormalities. Therefore, the lack of genomic instability is an important safety concern that can hamper studies with hiPSCs and their applications.

CRISPR/Cas9-induced DBS can be primarily repaired by either HDR or NHEJ [3, 35]. To obtain a precise genetic editing, HDR is the preferred pathway [4, 35], as the mutation we induced in the current study. The introduction of precise single base editions by HDR-mediated CRISPR/Cas9 into human *in vitro* models, such as hiPSCs, holds significant importance to study the functional impact of specific genetic alterations. This is imperative in the study of hereditary syndromes, where specific disease-relevant single nucleotide alterations are found in affected individuals [36]. Previous studies

have demonstrated that delivering a HDR donor DNA template can significantly improve the precision of repair, when comparing to traditional NHEJ [35]. Nevertheless, HDR presents a lower efficiency in most cells when compared to NHEJ, because it is restricted to the S and G2 phases of the cell cycle, when a homologous template is available [5]. Herein, we confirmed that HDR efficiency rate (6%) was considerably lower than NHEJ efficiency rate (47%). Thus, it is important to apply other strategies besides the donor DNA template that will allow cells to correct DNA through HDR to the detriment of NHEJ. Several studies have shown that, instead of inducing DSBs, which leads to correction by both HDR and NHEJ, inducing single-strand breaks favor HDR over NHEJ. This can be achieved by using nickase variants of Cas9 [37]. Furthermore, the low success rate of integrating the Cas9 vector into cells is a limitation in the present study. Although we present a very fast cell selection method with GFP+ cells being selected only 72 h after plasmid electroporation, our results still demonstrate that only in 2.5% of cells, the delivery of the Cas9 vector was successful. hiPSCs are known to be a challenging type of cells to perform CRISPR/Cas9. Furthermore, plasmid delivery techniques present an inherent toxicity to cells [15]. It is likely that many of the hiPSCs do not survive the successful delivery of the plasmid, resulting in death. Thus, improving the method to deliver Cas9 and sgRNA to the cells is an urgent need. It has been demonstrated that using Cas9-sgRNA ribonucleoprotein complexes (RNPs) instead of Cas9 plasmids holds significant improvements in genetic editing efficacy. A study performed by Xu and colleagues in 2021 demonstrated that using RNPs to introduce a 34 bp sequence in a hiPSC line resulted in a 40% efficiency [38]. Since the delivery occurs in a protein complex, it is not dependent on Cas9 translation, leading to a faster Cas9 activity [39]. Furthermore, RNPs have been shown to improve editing efficiency in hard-to-transfect cells [40], which is the case of hiPSC lines.

We successfully developed a *CTNNA1*: c.2023C>T (p.Q675*) homozygous isogenic hiPSC line using our CRISPR/Cas9 strategy, which further enabled us to understand the functional impact of this genetic alteration in non-differentiated cells. However, in certain disease contexts, obtaining a heterozygous cell line could be important. To achieve this, altering the cell sorting protocol from bulk to single cell sorting would be required. Our results demonstrate that inducing the *CTNNA1*: c.2023C>T (p.Q675*) homozygous nonsense alteration in a hiPSC line leads to a severe phenotype. Indeed, cells from clone #8, the homozygous edited cells containing the *CTNNA1*: c.2023C>T nonsense alteration, present an impacted capacity to form colonies and a severely impacted capacity to divide and proliferate. Nevertheless, other studies developed in our laboratory have demonstrated that homozygous editing of *CTNNA1* in terminally differentiated cells does not causes such a severe phenotype, pinpointing toward the important role of *CTNNA1/αE-catenin* proper expression in non-differentiated cells [41]. Studies have demonstrated that *αE-catenin* is a known critical molecule for cellular adhesion and signaling pathways that are essential for early development. In a mouse model, conditional knockout of murine *αE-catenin* homologue protein in epidermal cells led to extreme defects in skin, limbs and hair follicles of mice, displaying defects in adherens' junction formation, intercellular adhesion, and epithelial polarity [20]. Furthermore, previous research developed by us [41] and others [42] in *Drosophila* have shown that knockout of *Drosophila α-catenin* homologue protein often induces lethality. Supporting these observations, Sarpal and colleagues reported that *Drosophila α-catenin* null embryos cannot properly develop, leading to embryonic death [42]. This is consistent with an important role for *αE-catenin* in embryonic development, and pinpoints towards its

importance to maintain cultures of stable hiPSC lines. One limitation of this study is the direct consequence of the essential role of *CTNNA1* gene in mammalian cells. Although clone #8 presents the desired alteration in this study, with the severe impaired viability observed in this clone, no further analysis regarding RNA and protein were possible to perform.

Ultimately, with this study, we report an efficient method to obtain a precise genetic editing using HDR-mediated CRISPR/Cas9 in hiPSCs. The karyotyping protocol herein described is also an easy-to-implement, affordable protocol specifically tailored for the characterization of hiPSCs. This protocol offers researchers a streamlined and accessible alternative to outsourcing karyotyping to external companies, thus reducing dependency on third-party services and associated costs. By enabling in-lab assessment, this method empowers researchers to directly verify the genomic stability of their hiPSC lines, ensuring that the cells meet essential quality control standards for downstream applications. Due to its simplicity, our strategy can be further applied to different genes and different cell lines, including hard to edit cell lines.

Author contributions

Silvana Lobo (Conceptualization [equal], Data curation [equal], Formal analysis [equal], Investigation [equal], Methodology [equal], Validation [equal], Visualization [equal]), Rita Barbosa-Matos (Investigation [supporting], Methodology [supporting]), Sofia Dória (Investigation [supporting], Methodology [supporting]), Ana Pedro (Investigation [supporting], Methodology [supporting]), Ana Brito (Investigation [supporting], Methodology [supporting]), Daniel Ferreira (Investigation [supporting], Methodology [supporting], Supervision [supporting]), and Carla Oliveira (Conceptualization [equal], Data curation [equal], Formal analysis [equal], Funding acquisition [lead], Investigation [equal], Methodology [equal], Project administration [lead], Resources [lead], Supervision [lead], Validation [equal], Visualization [equal])

Supplementary data

Supplementary data is available at *Biology Methods and Protocols* online.

Funding

This work has received funding from the Fundação para a Ciência e Tecnologia from Portugal via a PhD studentship awarded to SL (REF: 2020.05773.BD). The work has been supported by the University of Porto through Doctoral Programme in Molecular and Cellular Biotechnology Applied to Health Sciences (ICBAS; awarded to SL), the Portuguese national funds through Fundação para a Ciência e Tecnologia, Ministério da Ciência, Tecnologia e Inovação (the DETONATE project Ref. 2022.02951.PTDC; the METAPREDICT project Ref.2023.12556.PEX; the HDGCHIP project Ref.#CI24-10293); the National Cancer Hub—Portugal (HDCHIP #NCH2024005), which is cofunded by Direção-Geral da Saúde through the National Program for Oncological Diseases and by the Agência de Investigação Clínica e Inovação Biomédica (AICIB), and the Portuguese Cancer League - Bolsa Nonô (REF: PEDIASCOPE). Salary to SL and RBM from the PREVENTABLE project (Grant Agreement No. 101095483) funded by the European Union's Horizon Europe.

Conflict of interest statement. None declared.

Data availability

The authors declare that all data supporting the findings of this study can be found within the article. Additional data supporting the findings of this study are available from the corresponding author upon request.

References

1. Doudna JA, Charpentier E. Genome editing. The new frontier of genome engineering with CRISPR-Cas9. *Science* 2014;**346**: 1258096. <https://doi.org/10.1126/science.1258096>
2. Hsu PD, Lander ES, Zhang F. Development and applications of CRISPR-Cas9 for genome engineering. *Cell* 2014;**157**:1262–78. <https://doi.org/10.1016/j.cell.2014.05.010>
3. Chang HHY, Pannunzio NR, Adachi N, Lieber MR. Non-homologous DNA end joining and alternative pathways to double-strand break repair. *Nat Rev Mol Cell Biol* 2017;**18**:495–506. <https://doi.org/10.1038/nrm.2017.48>
4. Ceccaldi R, Rondinelli B, D'Andrea AD. Repair pathway choices and consequences at the double-strand break. *Trends Cell Biol* 2016;**26**:52–64. <https://doi.org/10.1016/j.tcb.2015.07.009>
5. Jasin M, Haber JE. The democratization of gene editing: insights from site-specific cleavage and double-strand break repair. *DNA Repair (Amst)* 2016;**44**:6–16. <https://doi.org/10.1016/j.dnarep.2016.05.001>
6. Liu M, Rehman S, Tang X et al. Methodologies for improving HDR efficiency. *Front Genet* 2018;**9**:691. <https://doi.org/10.3389/fgene.2018.00691>
7. Elliott B, Richardson C, Winderbaum J et al. Gene conversion tracts from double-strand break repair in mammalian cells. *Mol Cell Biol* 1998;**18**:93–101. <https://doi.org/10.1128/mcb.18.1.93>
8. Kan Y, Ruis B, Takasugi T, Hendrickson EA. Mechanisms of precise genome editing using oligonucleotide donors. *Genome Res* 2017;**27**:1099–111. <https://doi.org/10.1101/gr.214775.116>
9. Song F, Stieger K. Optimizing the DNA donor template for homology-directed repair of double-strand breaks. *Mol Ther Nucleic Acids* 2017;**7**:53–60. <https://doi.org/10.1016/j.omtn.2017.02.006>
10. McBeath E, Parker-Thornburg J, Fujii Y et al. Rapid evaluation of CRISPR guides and donors for engineering mice. *Genes (Basel)* 2020;**11**:628. <https://doi.org/10.3390/genes11060628>
11. Takahashi K, Yamanaka S. Induction of pluripotent stem cells from mouse embryonic and adult fibroblast cultures by defined factors. *Cell* 2006;**126**:663–76. <https://doi.org/10.1016/j.cell.2006.07.024>
12. Chehelgerdi M, Behdarvand Dehkordi F, Chehelgerdi M et al. Exploring the promising potential of induced pluripotent stem cells in cancer research and therapy. *Mol Cancer* 2023;**22**:189. <https://doi.org/10.1186/s12943-023-01873-0>
13. Shi Y, Inoue H, Wu JC, Yamanaka S. Induced pluripotent stem cell technology: a decade of progress. *Nat Rev Drug Discov* 2017;**16**:115–30. <https://doi.org/10.1038/nrd.2016.245>
14. Niemitz E. Isogenic iPSC-derived models of disease. *Nat Genet* 2014;**46**:7. <https://doi.org/10.1038/ng.2864>
15. Rowe RG, Daley GQ. Induced pluripotent stem cells in disease modelling and drug discovery. *Nat Rev Genet* 2019;**20**:377–88. <https://doi.org/10.1038/s41576-019-0100-z>
16. Yoshihara M, Oguchi A, Murakawa Y. Genomic instability of iPSCs and challenges in their clinical applications. *Adv Exp Med Biol* 2019;**1201**:23–47. https://doi.org/10.1007/978-3-030-31206-0_2
17. Vaz IM, Borgonovo T, Kasai-Brunswick TH et al. Chromosomal aberrations after induced pluripotent stem cells

- reprogramming. *Genet Mol Biol* 2021;**44**:e20200147. <https://doi.org/10.1590/1678-4685-gmb-2020-0147>
18. Blair VR, McLeod M, Carneiro F et al. Hereditary diffuse gastric cancer: updated clinical practice guidelines. *Lancet Oncol* 2020; **21**:e386–e97. [https://doi.org/10.1016/s1470-2045\(20\)30219-9](https://doi.org/10.1016/s1470-2045(20)30219-9)
 19. Lobo S, Benusiglio PR, Coulet F et al. Cancer predisposition and germline CTNNA1 variants. *Eur J Med Genet* 2021;**64**:104316. <https://doi.org/10.1016/j.ejmg.2021.104316>
 20. Benusiglio PR, Colas C, Guillemin E et al. Clinical implications of CTNNA1 germline mutations in asymptomatic carriers. *Gastric Cancer* 2019;**22**:899–903. <https://doi.org/10.1007/s10120-018-00907-7>
 21. ISCN 2020: An International System for Human Cytogenomic Nomenclature (2020) Reprint of 'Cytogenetic and Genome Research 2020, Vol. 160, No. 7-8'. McGowan-Jordan J, Hastings RJ, Moore S, editors: S. Karger AG;2020 29 Oct 2020. <https://doi.org/10.1159/isbn.978-3-318-06867-2>
 22. Duboscq-Bidot L, Hoareau B, Ader F et al. Generation of CRISPR-Cas9 edited human induced pluripotent stem cell line carrying BAG3 V468M mutation in its BAG domain. *Stem Cell Res* 2024;**74**: 103294. <https://doi.org/10.1016/j.scr.2023.103294>
 23. Luo Y, Rao M, Zou J. Generation of GFP reporter human induced pluripotent stem cells using AAVS1 safe harbor transcription activator-like effector nuclease. *Curr Protoc Stem Cell Biol* 2014;**29**: 5a.7.1–18. <https://doi.org/10.1002/9780470151808.sc05a07s29>
 24. Yang L, Guell M, Byrne S et al. Optimization of scarless human stem cell genome editing. *Nucleic Acids Res* 2013;**41**:9049–61. <https://doi.org/10.1093/nar/gkt555>
 25. Andrews PW, Gokhale PJ. A short history of pluripotent stem cells markers. *Stem Cell Reports* 2024;**19**:1–10. <https://doi.org/10.1016/j.stemcr.2023.11.012>
 26. Paquet D, Kwart D, Chen A et al. Efficient introduction of specific homozygous and heterozygous mutations using CRISPR/Cas9. *Nature* 2016;**533**:125–9. <https://doi.org/10.1038/nature17664>
 27. Richardson CD, Ray GJ, DeWitt MA et al. Enhancing homology-directed genome editing by catalytically active and inactive CRISPR-Cas9 using asymmetric donor DNA. *Nat Biotechnol* 2016; **34**:339–44. <https://doi.org/10.1038/nbt.3481>
 28. Brinkman EK, Chen T, de Haas M et al. Kinetics and fidelity of the repair of Cas9-induced double-strand DNA breaks. *Mol Cell* 2018;**70**:801–13.e6. <https://doi.org/10.1016/j.molcel.2018.04.016>
 29. Asmamaw Mengstie M, Teshome Azezew M, Asmamaw Dejenie T et al. Recent advancements in reducing the off-target effect of CRISPR-Cas9 genome editing. *Biologics* 2024;**18**:21–8. <https://doi.org/10.2147/btt.S429411>
 30. Zhang XH, Tee LY, Wang XG et al. Off-target effects in CRISPR/Cas9-mediated genome engineering. *Mol Ther Nucleic Acids* 2015; **4**:e264. <https://doi.org/10.1038/mtna.2015.37>
 31. Guo C, Ma X, Gao F, Guo Y. Off-target effects in CRISPR/Cas9 gene editing. *Front Bioeng Biotechnol* 2023;**11**:1143157. <https://doi.org/10.3389/fbioe.2023.1143157>
 32. Nollet F, van Hengel J, Berx G et al. Isolation and characterization of a human pseudogene (CTNNA1) for alpha E-catenin (CTNNA1): assignment of the pseudogene to 5q22 and the alpha E-catenin gene to 5q31. *Genomics* 1995;**26**:410–3. [https://doi.org/10.1016/0888-7543\(95\)80231-a](https://doi.org/10.1016/0888-7543(95)80231-a)
 33. Karam R, Carvalho J, Bruno I et al. The NMD mRNA surveillance pathway downregulates aberrant E-cadherin transcripts in gastric cancer cells and in CDH1 mutation carriers. *Oncogene* 2008; **27**:4255–60. <https://doi.org/10.1038/onc.2008.62>
 34. Lykke-Andersen S, Jensen TH. Nonsense-mediated mRNA decay: an intricate machinery that shapes transcriptomes. *Nat Rev Mol Cell Biol* 2015;**16**:665–77. <https://doi.org/10.1038/nrm4063>
 35. Denes CE, Cole AJ, Aksoy YA et al. Approaches to enhance precise CRISPR/Cas9-mediated genome editing. *Int J Mol Sci* 2021;**22**: 8571. <https://doi.org/10.3390/ijms22168571>
 36. Kim HS, Kweon J, Kim Y. Recent advances in CRISPR-based functional genomics for the study of disease-associated genetic variants. *Exp Mol Med* 2024;**56**:861–9. <https://doi.org/10.1038/s12276-024-01212-3>
 37. Zhang J-P, Li X-L, Li G-H et al. Efficient precise knockin with a double cut HDR donor after CRISPR/Cas9-mediated double-stranded DNA cleavage. *Genome Biol* 2017;**18**:35. <https://doi.org/10.1186/s13059-017-1164-8>
 38. Xu H, Kita Y, Bang U et al. Optimized electroporation of CRISPR-Cas9/gRNA ribonucleoprotein complex for selection-free homologous recombination in human pluripotent stem cells. *STAR Protoc* 2021;**2**:100965. <https://doi.org/10.1016/j.xpro.2021.100965>
 39. Leal AF, Herreno-Pachón AM, Benincore-Flórez E et al. Current strategies for increasing knock-in efficiency in CRISPR/Cas9-based approaches. *Int J Mol Sci* 2024;**25**:2456. <https://doi.org/10.3390/ijms25052456>
 40. Goullée H, Taylor RL, Forrest ARR et al. Improved CRISPR/Cas9 gene editing in primary human myoblasts using low confluency cultures on Matrigel. *Skelet Muscle* 2021;**11**:23. <https://doi.org/10.1186/s13395-021-00278-1>
 41. Lobo S, Dias A, Ferreira M et al. 18P The role of CTNNA1 truncating variants in hereditary diffuse gastric cancer (HDGC). *Annals of Oncology* 2024;**35**:S220. <https://doi.org/10.1016/j.annonc.2024.08.027>
 42. Sarpal R, Pellikka M, Patel RR et al. Mutational analysis supports a core role for Drosophila α -catenin in adherens junction function. *J Cell Sci* 2012;**125**:233–45. <https://doi.org/10.1242/jcs.096644>